

# Semiconducting Polymers: A New Class of Solid-State Laser Materials

Fumitomo Hide, María A. Díaz-García, Benjamin J. Schwartz,\*  
Mats R. Andersson,† Qibing Pei, Alan J. Heeger

Gain narrowing in optically pumped thin films, both neat and undiluted, of luminescent conjugated polymers with different molecular structures was demonstrated. These results indicate that the polymers studied have large cross sections for stimulated emission, that population inversion can be achieved at low pump energies, and that the emitted photons travel distances greater than the gain length within the gain medium. The use of simple waveguide structures is sufficient to cause low gain narrowing thresholds in submicrometer-thick films.

Many conjugated polymers are luminescent materials with emission that is shifted sufficiently far from the absorption edge that self-absorption is minimal. Because of the large joint density of states associated with the direct  $\pi$  to  $\pi^*$  (interband) transition of these quasi-one-dimensional semiconducting polymers, the absorption coefficient ( $\alpha$ ) is large, typically  $\alpha \approx 10^5 \text{ cm}^{-1}$  (1). To first order, the cross section for stimulated emission (SE) is the same as that for absorption, so the gain length should be essentially equal to the absorption length scaled by the fraction of chromophores in the excited state (2). An inverted population can be achieved by simply pumping the  $\pi$  to  $\pi^*$  transition; this process does not simultaneously stimulate emission because the absorption and emission are spectrally separated. Thus, semiconducting luminescent polymers offer promise as novel laser materials with gain lengths in the micrometer or submicrometer regime.

A variety of optoelectronic devices have been demonstrated in which conjugated polymers are used as the active semiconducting materials, including diodes (3), light-emitting diodes (4), photodiodes (5), field-effect transistors (6), polymer grid triodes (7), and light-emitting electrochemical cells (8). Notably absent from this list of conjugated polymer devices, however, is the semiconducting polymer injection laser. Laser emission has been observed from poly(2-methoxy-5-(2'-ethyl-hexyloxy)-1,4-phenylene vinylene), MEH-PPV, in dilute so-

lution in an appropriate solvent, in direct analogy with conventional dye lasers (9). An optically pumped polymer laser was recently demonstrated in which the gain material was a dilute blend of MEH-PPV (<1%) in polystyrene (PS) (10); these thick ( $\sim 100 \mu\text{m}$ ) films contain a dispersion of  $\text{TiO}_2$  nanoparticles that confine the emitted photons by multiple scattering so that the distance traveled in the medium exceeds the gain length.

Although ultrafast spectroscopy has been used to demonstrate SE in dilute solutions and dilute blend films containing conjugated polymers, the SE in neat films either does not exist (11) or decays in at most a few picoseconds (12). This absence of SE results from interchain interactions that give rise to photoinduced absorption strong enough to overwhelm the SE. We recently discovered, however, that in neat films of BuEH-PPV (see Table 1 for full chemical name and Fig. 1A for molecular structure), SE persists for more than 60 ps (13), nearly an order of magnitude longer than that reported previously for other polymers. This result demonstrates the possibility of synthesizing semiconducting polymers with long SE lifetimes by a judicious choice of functionalized side chains on the polymer backbone and indicates that such polymers can be considered as candidates for laser materials.

In this report, luminescent conjugated polymers are shown to have gain narrowing as neat films of submicrometer thickness, including polymers with the backbone molecular structures of poly(*p*-phenylenevinylene) (PPV) (14), poly(*p*-phenylene) (PPP) (15), and polyfluorene (PF) (16). The instrumentation for gain narrowing experiments with thin solid films has been described in detail elsewhere (10). Light emission was typically collected from the front face of the sample, but lasing could be detected in all directions (the spectral profiles do not depend on angle either at low pump energies or above threshold). The

excitation source (the pump) was a 10-Hz, Q-switched Nd:YAG (yttrium-aluminum-garnet) laser that provided  $\sim 10$ -ns pulses at 532 and 355 nm, focused to  $\sim 1$  mm. The first anti-Stokes Raman line (435 nm) from a high-pressure  $\text{H}_2$  cell pumped at 532 nm was also used. The energy per pulse was controlled with calibrated neutral density filters.

The photoluminescence (PL) spectrum evolution for a neat film of BuEH-PPV (210-nm thick) is shown as a function of the pump energy per pulse in Fig. 1A. As the pump energy is increased, a gain-narrowed peak rises out of the broad emission spectrum. At sufficiently high energies, only the gain-narrowed peak survives while the broad tails of the PL are completely suppressed. This dramatic collapse of the line width (17) (from 130 nm to 9 nm) at remarkably low pump energies ( $\leq 1 \mu\text{J}$  per pulse) implies a very short gain length. A blue shift of the emission peak at higher energies is also evident in Fig. 1A, which suggests that SE occurs on a time scale

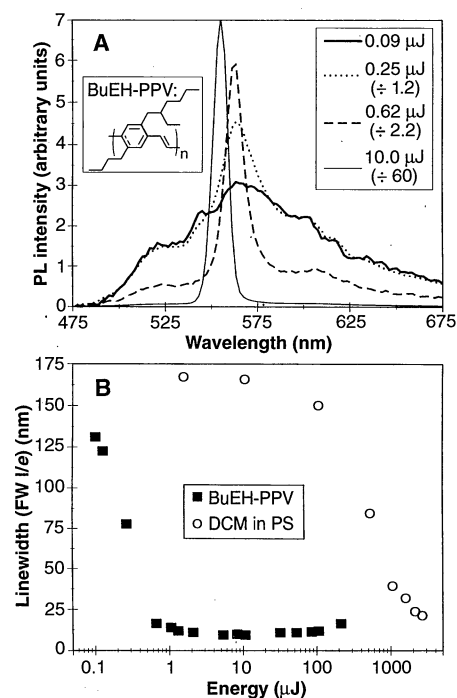


**Fig. 1.** (A) Photoluminescence spectrum of 210-nm-thick BuEH-PPV neat film on glass (spin cast from *p*-xylene solution) at various pump pulse energies both above (10.0  $\mu\text{J}$ , thin solid curve; 0.62  $\mu\text{J}$ , dashed curve) and below (0.25  $\mu\text{J}$ , dotted curve; 0.09  $\mu\text{J}$ , thick solid curve) the lasing threshold. **Inset:** Chemical structure of BuEH-PPV. (B) Evolution of the linewidth [full-width (FW) at 1/e height] as a function of pump pulse energy (on a logarithmic scale) for the BuEH-PPV sample of (A) (squares) and for comparison a 2.6 weight percent film of DCM laser dye in PS (open circles) of 3600-nm thickness with comparable optical density to the BuEH-PPV film.

F. Hide, M. A. Díaz-García, B. J. Schwartz, M. R. Andersson, A. J. Heeger, Institute for Polymers and Organic Solids, University of California, Santa Barbara, Santa Barbara, CA 93106-5090, USA.  
Q. Pei, UNIAX Corporation, 6780 Cortona Road, Santa Barbara, CA 93117, USA.

\*Present address: Department of Chemistry and Biochemistry, University of California, Los Angeles, CA 90095-1569, USA.

†Present address: Departments of Organic Chemistry and Polymer Technology, Chalmers University of Technology, S-412 96, Göteborg, Sweden.

faster than the spectral diffusion that occurs during the first few tens of picoseconds after photoexcitation (10). The linewidth of the PL as a function of pump pulse energy (Fig. 1B) shows a well-defined threshold.

If the gain lengths are indeed in the micrometer or submicrometer regime, the energy threshold for gain narrowing should be much lower than for conventional laser materials. For reference, we tested the laser dye DCM (18) (see Table 1) suspended in films of PS with optical densities comparable to those of the 210-nm BuEH-PPV film of Fig. 1. Although these DCM concentrations are more than two orders of magnitude higher than in typical dye lasers, the threshold for gain narrowing is more than 1000 times greater than that of BuEH-PPV (Fig. 1B). Thus, conjugated polymers provide the intense absorption and emission characteristics of organic dyes but with the substantial advantage of having a much higher density of chromophores in the solid state. Moreover, because conjugated polymers are semiconductors, our results demonstrate the possibility for producing electrically pumped polymer diode lasers.

We have exploited gain narrowing from a number of PPV derivatives (19) and from polymers with the PPP and PF backbone structures; the corresponding  $\pi$ - $\pi^*$  energy gaps span the visible spectrum. The chemical structure, excitation wavelength, peak emission, energy threshold for line narrowing, and narrowed linewidth for thin films of these various semiconducting polymers are summarized in Table 1 (20). The very

low energy thresholds lead us to conclude that semiconducting polymers comprise a class of promising laser materials.

The data in Fig. 2 demonstrate the advantages of the high density of chromophores characteristic of semiconducting polymers. The linewidths versus pump energy of films of varying BCHA-PPV (see Table 1 for complete name) concentrations diluted in PS are shown in Fig. 2. Upon increasing the concentration of BCHA-PPV in the film from 8.4% to 100% (a factor of 12), the threshold energy decreased by three orders of magnitude, to a minimum of 1.3  $\mu$ J per pulse for the neat film. This strongly superlinear behavior may be indicative of coherent emission from the BCHA-PPV (21).

We performed additional experiments to measure the effects of the film thickness and to determine the role of possible confinement through waveguiding of the emitted light. These experiments support a picture of lasing in conjugated polymer films with submicrometer thicknesses aided by rudimentary waveguiding in either the polymer film or the substrate.

The thickness dependence of gain narrowing was studied for neat films of three different conjugated polymers, BuEH-PPV, BCHA-PPV, and MEH-PPV, as well as for the reference films of DCM in PS films (Table 1). Films of various thicknesses were prepared by spin casting. For each polymer, a well-defined thickness cutoff is observed below which gain narrowing does not occur. The existence of such a cutoff suggests a

waveguiding effect. The polymer films actually constitute simple asymmetric planar waveguides because the refractive indices ( $n$ ) at the emission wavelength for all of the polymers studied ( $1.56 \leq n_{\text{polymer}} \leq 2.0$ ) (22) are greater than those of the surrounding media ( $n_{\text{glass}} = 1.52$  and  $n_{\text{air}} = 1.0$ ). Therefore, for sufficiently thin films, a guided mode cannot be supported; that is, a minimum thickness cutoff condition exists for propagation of a guided mode (23). For all three polymers, the minimum thicknesses required to propagate the fundamental mode through the films, as calculated from their known refractive indices, agree well with the thickness thresholds below which gain narrowing was not experimentally observed. Thus, waveguiding in the thin film structures confines the emitted photons and leads to low gain narrowing thresholds for submicrometer thick films (24).

Additional experiments were performed to confirm the waveguiding hypothesis. First, a BuEH-PPV/glass sample which was too thin (43 nm) to show line narrowing as an asymmetric waveguide in air was immersed in a solvent that was approximately index-matched to the glass substrate (cyclohexanone,  $n = 1.45$ ). This produced a configuration with a symmetric waveguide structure (glass-polymer-solvent) in which no minimum film thickness for waveguiding is expected (23). Once in the solvent, the film showed dramatic line narrowing. This process is reversible: removing the film from the index-matched solvent causes the laser behavior to disappear.

**Table 1.** Properties of semiconducting polymer films. Sh, shoulder; Th, thickness.

Material	Peak PL emission (nm)	$\lambda_{\text{pump}}$ (nm)	Energy threshold ( $\mu$ J/pulse)	Final linewidth (nm)	Film thickness (nm)	Cutoff thickness (nm)	Solvent
BuEH-PPV*	520, 560	435	0.4 $\pm$ 0.2	12	126–252	106 $\leq$ Th $\leq$ 126	THF
BCHA-PPV†	540, 630 (Sh)	532	0.2 $\pm$ 0.1	9	87–208	65 $\leq$ Th $\leq$ 87	<i>p</i> -xylene
MEH-PPV‡	585, 625	532	1.0 $\pm$ 0.4	11	277–650	160 $\leq$ Th $\leq$ 277	THF
			1.1 $\pm$ 0.4	17	87–405	53 $\leq$ Th $\leq$ 87	THF
			3	50	355	<355	CB
			4	55	325	<325	<i>p</i> -xylene
BEH-PPV§	580, 650	532	0.5	13	300	<300	THF
M3O-PPV	530, 620	532	4	16	310	<310	THF
BuEH-MEH copolymers¶							
10:90	580, 625	532	3.2	23	330	<330	THF
70:30	565, 600	532	1.0	15	420	<420	THF
90:10	550, 580 (Sh)	435	1.0	20	370	<370	THF
95:5	545, 580 (Sh)	435	1.6	20	450	<450	THF
97.5:2.5	540, 570 (Sh)	435	1.0	18	500	<500	THF
HEH-PF#	425, 445	355	4.2	12	120	<120	THF
BDOO-PF**	430, 450, 540	355	2.3	7			THF
CN-PPP††	420	355	4	12	100	<100	THF
DCM/PS‡‡ (2.6% w/v)	640	532	400 $\pm$ 150	23	390–4800	260 $\leq$ Th $\leq$ 390	THF

\*Poly(2-butyl-5-(2'-ethylhexyl)-1,4-phenylene vinylene); see Fig. 1A inset. †Poly(2,5-bis(cholestanoxy)-1,4-phenylene vinylene). ‡Poly(2-methoxy-5-(2'-ethylhexyloxy)-1,4-phenylene vinylene); see Fig. 3 inset. §Poly(2,5-bis(2'-ethylhexyloxy)-1,4-phenylene vinylene). ||Poly(2-methoxy-5-(3'-octyloxy)-1,4-phenylene vinylene). ¶Copolymers synthesized from varying ratios of BuEH-PPV and MEH-PPV monomers. #Poly(9-hexyl-9-(2'-ethylhexyl)-fluorene-2,7-diyl). \*\*Poly(9,9-bis(3,6-dioxoacetyl)-fluorene-2,7-diyl). ††Poly(2-(6'-cyano-6'-methylheptyloxy)-1,4-phenylene). ‡‡4-(dicyanomethylene)-2-methyl-6-(4-dimethylaminostyryl)-4H-pyran.

Second, the waveguide was altered by choosing a different substrate. BuEH-PPV films ( $n = 1.70$ ) on optically flat sapphire substrates ( $n = 1.76$ ) in the standard configuration (pumping directly over the film) showed only limited gain narrowing. However, exciting the film through the sapphire led to strong gain narrowing. This effect can be understood in terms of waveguiding in the substrate: Because  $n$  of the substrate is greater than that of the film, some of the emitted light that travels into the substrate will be guided by multiple reflections in the substrate. However, the evanescent wave that penetrates from the substrate into the excited film can be amplified. Pumping from the top of the film does not sufficiently excite the polymer near the substrate interface where the guided evanescent wave penetrates; pumping through the substrate is an ideal configuration. To confirm this hypothesis, a BuEH-PPV/sapphire film that showed gain narrowing with a low threshold was immersed in a high-index solvent, diiodomethane ( $n = 1.75$ ). Because this solvent is approximately index-matched to sapphire, the waveguiding effect is expected to disappear. In fact, regardless of the pumping geometry, the gain narrowing was inhibited when this film was immersed in the high-index solvent. These waveguiding results are consistent with previous work on dye-doped sol-gel composites, where similar phenomena were observed (25).

Film morphology and chain conformation also play a role, as shown by spin-casting neat films of BuEH-PPV and MEH-PPV on glass from different solvents. BuEH-PPV films cast from tetrahydrofuran (THF) or from *p*-xylene show the same behavior, with similar threshold energies for gain narrowing and with similar final line widths

(see Table 1). For MEH-PPV films, however, the gain narrowing is strongly dependent on the choice of solvent (Fig. 3). Films cast from THF show a narrow final linewidth (17 nm) in contrast with the broad final widths ( $\geq 50$  nm) obtained for films cast from chlorobenzene (CB) or *p*-xylene, even under strong pumping conditions. In addition, the threshold for what little line narrowing takes place in films cast from the aromatic solvents is  $\sim 5$  times greater than in films cast from THF. The latter results are intriguing in light of previous ultrafast spectroscopic data that showed no SE from neat films of MEH-PPV cast from CB (11). Thus, solvent dependence of chain packing appears to offer an alternative way to control or enhance SE.

We have observed clear evidence of gain narrowing with a low pump-energy threshold, in submicrometer-thick semiconducting polymer films. The question is whether these data are indicative of lasing, amplified spontaneous emission (ASE), or superradiance. More detailed experiments are required to resolve these issues. We emphasize, however, that the low threshold gain narrowing is observed only when the polymer film is in the form of a waveguide, that is, only when the active medium is coupled to a simple resonant structure.

The observation of gain narrowing in optically pumped neat films of this class of conjugated polymers with the aid of simple waveguiding provides incentive to pursue the use of conjugated polymers as laser materials. Microlasers made with gain media consisting of transparent polymer hosts doped with efficient fluorescent dyes in well-defined cavities have been demonstrated (26). However, despite attempts to construct high-Q resonant cavities with conjugated polymers (27), laser

emission has not been reported from neat thin films until recently (28), primarily because of the lack of SE in the materials being studied. Because the threshold for gain narrowing is much lower for appropriately chosen conjugated polymers (see Fig. 1B and Table 1), the benefits of combining the micrometer or submicrometer gain lengths characteristic of neat, undiluted films of luminescent conjugated polymers with high-Q cavities are obvious. Sophisticated, high-Q structures such as distributed feedback (DFB) or distributed Bragg reflectors (DBR) can be used; in fact, lasing has been reported from thin films of poly(*p*-phenylenevinylene) in a DBR microcavity (28). The achievement of electrically pumped solid-state lasers with such polymers as the active gain medium is an important goal. Because submicrometer thin films are required for bright electroluminescence (EL) in polymer diodes (29), electrically pumped solid-state lasers will require semiconductor laser materials with submicrometer gain lengths. Although luminescent polymers can satisfy this requirement, carrier concentrations sufficient to produce laser action must be produced by electrical pumping. For the photon densities in the luminescent film at threshold (see Table 1) and assuming a 5% internal quantum efficiency for EL, the transient current densities necessary to reach the threshold for gain narrowing may be in excess of thousands of amperes per square centimeter. The current required can be decreased by utilizing relatively high-Q resonant structures (such as microcavities, or distributed feedback). Because current densities of 25 A/cm<sup>2</sup> have been reported in electrically pulsed MEH-PPV diodes ( $4 \times 10^{-3}$  cm<sup>2</sup> area) when operated with 3- $\mu$ s pulses at low duty cycle (30), sufficiently high current densities should be accessible with small active areas and low duty cycles, especially when aided by improvements in EL efficiency and improvements in thermal management.

REFERENCES AND NOTES

1. A. J. Heeger, S. Kivelson, J. R. Schrieffer, W.-P. Su, *Rev. Mod. Phys.* **60**, 781 (1988).
2. A. Yariv, *Quantum Electronics* (Wiley, New York, ed. 3, 1989), chap. 8.
3. H. Tomozawa, D. Braun, S. Phillips, A. J. Heeger, H. Kroemer, *Synth. Met.* **22**, 63 (1987).
4. J. H. Burroughes *et al.*, *Nature* **347**, 539 (1990); D. Braun and A. J. Heeger, *Appl. Phys. Lett.* **58**, 1982 (1991); G. Gustafsson *et al.*, *Nature* **357**, 477 (1992).
5. G. Yu and A. J. Heeger, *J. Appl. Phys.* **78**, 4510 (1995); J. J. M. Halls *et al.*, *Nature* **376**, 498 (1995); G. Yu, J. Gao, J. C. Hummelen, F. Wudl, A. J. Heeger, *Science* **270**, 1789 (1995).
6. J. H. Burroughes, C. A. Jones, R. H. Friend, *Nature* **335**, 137 (1988); F. Garnier, R. Hajlaoui, A. Yasser, P. Srivastava, *Science* **265**, 1684 (1994); A. R. Brown, A. Pomp, C. M. Hart, D. M. de Leeuw, *ibid.* **270**, 972

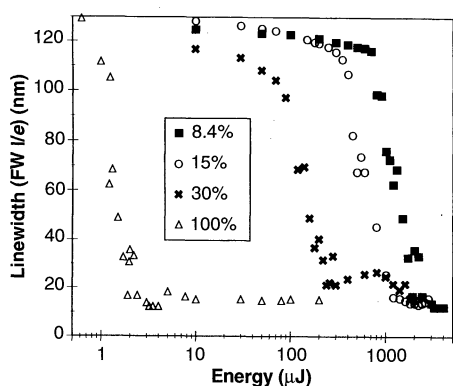


Fig. 2. Emission linewidth as a function of pump pulse energy (on a logarithmic scale) for various BCHA-PPV/PS blend films at different BCHA-PPV concentrations: 8.4% (squares), 15% (open circles), 30% (crosses), and neat (100%) (open triangles).

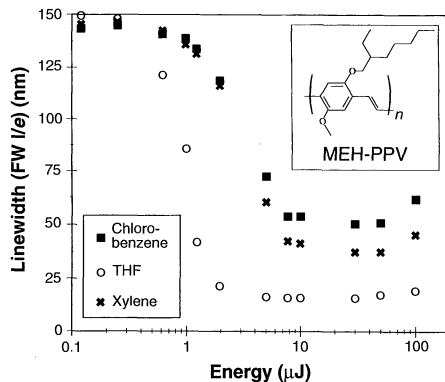


Fig. 3. Emission linewidth as a function of pump pulse energy (on a logarithmic scale) for MEH-PPV neat films cast on glass from different solvents: tetrahydrofuran (open circles); *p*-xylene (crosses); and chlorobenzene (squares). Inset: Chemical structure of MEH-PPV.

# Nanorod-Superconductor Composites: A Pathway to Materials with High Critical Current Densities

Peidong Yang and Charles M. Lieber\*

- (1995); L. Torsi, A. Dodabalapur, L. J. Rothberg, A. W. P. Fung, H. E. Katz, *ibid.* **272**, 1462 (1996).
7. Y. Yang and A. J. Heeger, *Nature* **372**, 344 (1994).
  8. Q. Pei, G. Yu, C. Zhang, Y. Yang, A. J. Heeger, *Science* **269**, 1086 (1995); Q. Pei, Y. Yang, G. Yu, C. Zhang, A. J. Heeger, *J. Am. Chem. Soc.* **118**, 3922 (1996); Y. Cao, G. Yu, A. J. Heeger, C. Y. Yang, *Appl. Phys. Lett.* **68**, 3218 (1996).
  9. D. Moses, *Appl. Phys. Lett.* **60**, 3215 (1992).
  10. F. Hide, B. J. Schwartz, M. A. Diaz-Garcia, A. J. Heeger, *Chem. Phys. Lett.* **256**, 424 (1996).
  11. M. Yan, L. J. Rothberg, E. W. Kwock, T. M. Miller, *Phys. Rev. Lett.* **75**, 1992 (1995).
  12. M. Yan *et al.*, *ibid.* **72**, 1104 (1994); R. Kersting *et al.*, *ibid.* **70**, 3820 (1993); W. Graupner *et al.*, *ibid.* **76**, 847 (1996); T. Pauck *et al.*, *Chem. Phys. Lett.* **244**, 171 (1995).
  13. B. J. Schwartz, F. Hide, M. R. Andersson, A. J. Heeger, in preparation.
  14. C. Zhang, S. Höger, K. Pakbaz, F. Wudl, A. J. Heeger, *J. Electron. Mater.* **22**, 413 (1993); C. L. Gettinger, A. J. Heeger, J. M. Drake, D. J. Pine, *J. Chem. Phys.* **101**, 1673 (1994).
  15. Y. Yang, Q. Pei, A. J. Heeger, *J. Appl. Phys.* **79**, 934 (1996).
  16. Q. Pei and Y. Yang, *J. Am. Chem. Soc.* **118**, 7416 (1996). For past polyfluorene work, see Y. Ohmori, M. Uchida, C. Morishima, A. Fujii, K. Yoshino, *Jpn. J. Appl. Phys.* **32**, L1663 (1993).
  17. We have chosen the full-width at 1/e height to represent the linewidth of the emission spectra because this is more suitable (compared to other definitions such as FWHM) for comparison of disparate emission spectra with varying magnitudes of vibronic features.
  18. P. R. Hammond, *Opt. Commun.* **29**, 331 (1979).
  19. Among the PPV derivatives are several copolymers synthesized from varying ratios of BuEH-PPV and MEH-PPV monomers.
  20. Details of film preparation and characterization will be reported elsewhere; B. J. Schwartz, M. A. Diaz-Garcia, F. Hide, A. J. Heeger, in preparation.
  21. We thank Z. V. Vardeny for making this point clear.
  22. Polymer refractive indices were determined from the waveguide modal characterization by the prism coupling technique. We also note that the polymer films are birefringent and have a higher index in the plane of the substrate, which is indicative of partial chain alignment. See (20) for details.
  23. H. Kogelnik, in *Topics in Appl Optics: Integrated Optics*, T. Tamir, Ed. (Springer-Verlag, Berlin, 1979), vol. 7, chap. 2.
  24. Although absolute measurements of the PL quantum efficiency are difficult because the films are acting as waveguides, the integrated area of the PL data in Fig. 1 increases sublinearly at high pump energies. This sublinear increase might arise from excitation quenching at high excitation densities above threshold (28).
  25. D. Shamrakov and R. Reisfeld, *Chem. Phys. Lett.* **213**, 47 (1993).
  26. M. Kuwata-Gonokami *et al.*, *Opt. Lett.* **20**, 2093 (1995).
  27. J. Grüner, F. Cacialli, R. H. Friend, *J. Appl. Phys.* **80**, 207 (1996); V. Cimrová and D. Neher, *ibid.* **79**, 3299 (1996); M. Berggren *et al.*, *Synth. Met.* **76**, 121 (1996); T. A. Fisher *et al.*, *Appl. Phys. Lett.* **67**, 1355 (1995); H. F. Wittman *et al.*, *Adv. Mater.* **7**, 541 (1995).
  28. R. H. Friend, paper presented at the International Conference on Science and Technology of Synthetic Metals (ICSM '96), Snowbird, UT, 31 July 1996.
  29. I. D. Parker, *J. Appl. Phys.* **75**, 1656 (1994).
  30. D. Braun, D. Moses, C. Zhang, A. J. Heeger, *Appl. Phys. Lett.* **61**, 3092 (1992).
  31. We thank G. Yu and Y. Yang (UNIAX Corp.) for valuable assistance and discussions, and UNIAX Corp. for making the Dektak surface profilometer available. Supported by the Office of Naval Research (N00014-91-J-1235). M.A.D.-G. is supported by the Government of Spain. M.R.A. thanks the Swedish Natural Science Research Council for support.

Most large-scale applications of the high-temperature copper oxide superconductors (HTSCs) require high critical current densities ( $J_c$ 's) at temperatures near the boiling point of liquid nitrogen to be technologically useful, although thermally activated flux flow reduces  $J_c$  dramatically at these temperatures. This intrinsic limitation can be overcome by introducing nanometer-sized columnar defects into an HTSC. Nanorods of magnesium oxide were grown and incorporated into HTSCs to form nanorod-HTSC composites. In this way, a high density of nanorod columnar defects can be created with orientations perpendicular and parallel to the copper oxide planes. The  $J_c$ 's of the nanorod-HTSC composites are enhanced dramatically at high temperatures and magnetic fields as compared with reference samples; these composites may thus represent a technologically viable strategy for overcoming thermally activated flux flow in large-scale applications.

Large  $J_c$ 's are essential to many proposed applications of HTSCs, such as wires for power transmission cables and solenoids (1, 2). In general,  $J_c$  is limited by two major factors (1, 3, 4). First,  $J_c$  is limited by thermally activated flux creep; that is,  $J_c$  vanishes well below the upper critical field line  $H_{c2}(T)$  (which depends on temperature  $T$ ) as a result of the motion of magnetic flux lines. This limitation is intrinsic and arises from the short coherence lengths and large anisotropies of the HTSC materials that lead to a weak pinning of flux lines (3–6). Second, in polycrystalline materials,  $J_c$  is limited by the alignment of the interfaces between superconducting grains: poor alignment of the grains and chemical heterogeneity at their boundaries produces weak links with low values of  $J_c$  (3, 7). Progress has been made in improving the alignment of grains and consequently improving  $J_c$ 's in wires and tapes based on  $\text{Ag-Bi}_2\text{Sr}_2\text{Ca}_{n-1}\text{Cu}_n\text{O}_{2n+4}$  ( $n = 2$ , BSCCO-2212;  $n = 3$ , BSCCO-2223) through investigations of the effects of different material processing conditions on microstructure and on microscopic and macroscopic transport currents (3, 8–10). Despite this progress in processing, which is now yielding BSCCO-based wires with  $J_c$  values sufficiently high to be considered for some commercial applications (9), the intrinsic problem of thermally activated flux creep continues to limit the performance of BSCCO materials at high  $T$  and  $H$  (11–13).

Theoretical (14, 15) and experimental (16, 17) studies have shown, however, that

this problem in HTSCs can be reduced by creating correlated defects, such as columnar defects, in the crystal lattice. The interaction of flux lines with columnar defects results in a large pinning energy that effectively resists thermally activated flux motion and thus increases  $J_c$  significantly at high  $T$  and  $H$  (14, 18). These linelike defects are usually created by irradiating samples with heavy ions having energies on the order of a gigavolt (Fig. 1). This procedure yields damage tracks 10 to 20 nm in diameter and tens of micrometers in length (19). The small defect diameter is essential to maximize the flux line core-pinning interaction without destroying an unne-

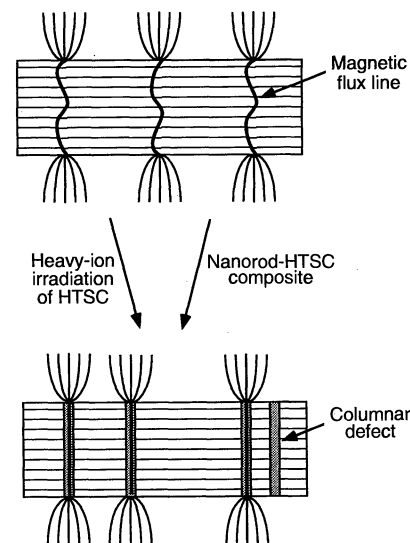


**Fig. 1.** Schematic diagram illustrating magnetic flux lines in an HTSC before and after the creation of columnar defects. The linear columnar defects strongly trap or pin the flux lines in the superconductor.

P. Yang, Department of Chemistry, Harvard University, Cambridge, MA 02138, USA.

C. M. Lieber, Division of Applied Sciences and Department of Chemistry, Harvard University, Cambridge, MA 02138, USA.

\*To whom correspondence should be addressed.

12 July 1996; accepted 27 August 1996